Received: October 23, 2020. Revised: January 14, 2021. 344

International Journal of
Intelligent Engineering & Systems

http://www.inass.org/

Cellular Communication-Based Autonomous UAV Navigation with Obstacle Avoidance for Unknown Indoor Environments

Yeon Ji Choi[1] **I Nyoman Apraz Ramatryana**[1] **Soo Young Shin**[1]*

[1] *Department of IT Convergence Engineering, Kumoh National Institute of Technology, 61 Daehak-ro, Gumi, Gyeongbuk, 39177, South Korea*
* Corresponding author's Email: wdragon@kumoh.ac.kr

Abstract: The technology of Unmanned Aerial Vehicles (UAV) has been the subject of pioneering research in recent years. Also, the subject has been used in various situations for both outdoor and indoor. In this paper, a cellular communication-based autonomous UAV Navigation is proposed that enables UAVs to maneuver independently in previously unknown and GPS-denied indoor environments with LiDAR sensors. The main idea of the proposed scheme is to implement LTE connection to UAV Navigation and compared it to a Wi-Fi connection. We have proposed that autonomous UAV navigation system for unknown environment like indoor. This system relies on the combination of ROS-based Hector SLAM systems, 2D-LiDAR sensor and LTE connection. The performance of proposed scheme is evaluated as the error distance and exploration time for unknown area like indoor environment. The mapping efficiency of LTE connection is 57.5% greater than the Wi-Fi connection. Computation time for flight is approximately 200 seconds.

Keywords: Autonomous UAV, Navigation, SLAM, Obstacle avoidance, LiDAR sensor, LTE connection, Unknown indoor environment.

1. Introduction

In many fields such as air defense, precision agriculture, militaries, smart transport, searches and rescue operations and many other sectors, unmanned aerial vehicles (UAV) have become substantially established in the scientific world. Also, The UAVs have been used in various environments for both outdoor and indoor, including reconnaissance, surveillance, saving lives in disaster situations, indoor positioning and utilization in logistics warehouses. There has been considerable progress in the autonomous navigation of these systems. The global positioning system (GPS) is used for external autonomous navigation [1]. Because GPS signals are typically absent or weak indoors, autonomous navigation is difficult [2].

There are various approaches for independent indoor navigation which have been proposed in recent years. In most of them, laser range detectors (LiDAR) [3], RGB-D sensors [4], or stereo vision [5] are used to create a 3D map of an unseen field, which helps to locate the unit at all times. Simultaneous localization and mapping (SLAM) technology is used by the unit to construct an indoor map in real time and simultaneously locate its own position on the map. A point cloud map of the indoor environment is used for SLAM technology. The cloud map can be applied to several fields, such as surveying and mapping, which significantly improves the effectiveness of building indoor maps.

However, it is an intensively computational method in most real-time scenarios and thus fails. When a UAV acquires a map and compute scenarios in real-time simultaneously various positioning and mappings algorithms have been used for theoretical analysis and practical applications in the fields of robotics [6]. This is challenging point for solving practical these problems. The challenge of selecting an algorithm involves comparing the relevant methods and choosing the appropriate one. The most significant problem is that the SLAM algorithm is

typically difficult to set up in a private setting. Due to this problem, a modular architecture has been developed for running robot applications using the robot operating system (ROS). The concept of the ROS indicates to create a machine that could be used by modifying a small amount of code on many robotic systems. The ROS also helps researchers simulate easily and perform real experiments effectively. The ROS application programming interface is provided by most SLAM libraries. The most commonly used LiDAR SLAM libraries are Gmapping [7], Google Cartographers [8] and Hector SLAM [9].

Previous reports [10, 11] include trajectory comparisons, which are measured via LiDAR-based SLAM trajectories with data obtained using various visible sensors (stereo and monocular cameras) and laser (depth sensors). An analysis [12] was performed on five laser 2D SLAM techniques usable in ROS for data obtained in real-life testing, using the following maps created with measurements based on local neighborhoods: Hector SLAM, Gmapping, KartoSLAM, CoreSLAM and LagoSLAM. In another study, three 2D SLAM methods provided by the ROS were compared: Gmapping, Hector SLAM and CRSM SLAM [13]. These studies motivated us to support and improve the 2D SLAM methodical study of the Gmapping, Hector SLAM and Google Cartographers with [12] average nearest neighbor distance (ANND) metrics. Accordingly, this paper proposes cellular-communication-based connection for an autonomous UAV with a LiDAR sensor and Hector SLAM. The communication has decided as long term evolution (LTE) which is cellular-based connection.

The rest of the work is organized as Section 2 details the related work, while section 3 explains the system model and implementation. Section 4 includes the experimental results and discussion. Section 5 wraps the work with a conclusion and future work.

2. Related works

In previous studies on autonomous UAV navigation, a 3D map of the local area has constructed. These techniques are used in certain situations to map precise trajectories for quadcopters [14, 15]. However, they are based on a sophisticated control regime and thus their use is limited to laboratory settings [16, 17, 18]. In other methods, the map is learned from a manual path and quadcopters fly along the same path [19]. GPS-based posing projections are used for most outdoor flights that are not as accurate indoor scenarios.

All approaches employ small size sensors, such as infrared, RGB-D or laser spectrum sensors [4]. For an autonomous navigation systems, a single ultrasonic sensor is used with an infrared sensor [20]. The LiDAR and inertial measurement unit (IMU) state assessment approach indicate stable operation in an unknown environment that are refuted by a GPS [21]. The problem with range sensors is that they are heavy and their power consumption is high and thus they are not ideal for most UAVs.

The SLAM technique uses various optical sensors for generating a 3D map [16-18] with the location of a UAV at any point on the map [22]. A 3D map of an uncertain indoor scenario is used for the SLAM using a laser rangefinder [23]. Indoor navigation with a single camera is achieved using the SLAM technique [24, 25]. However, the major downside of SLAM is that the regeneration of the 3D map area is complex, requiring considerably high-precision measurement and resource usage, as additional sensors are necessary.

In the case of real-time navigation, SLAM can also generate communication delays and small size maps [26, 27]. Moreover, SLAM is primarily a feature-based device and its performance is poor for indoor materials, such as walls/roofs, because of its inadequate differential strength. In a hallway consisting of walls, roofs and floors, the SLAM technology cannot achieve a desirable navigational efficiency.

3. System model and implementation

Navigation is a technique for controller and deciding moving paths and direction from a environment map for localization. There are three types of navigation: map building-based, map-based and map-less. In the present study, map building-base method have used regarding the unknown environment in this paper. It allows UAVs to create their own maps from sensing information through SLAM. The occupancy map divides the space into a grid of a certain size. The free space for flying UAV is distinguished from the space occupied by obstacles

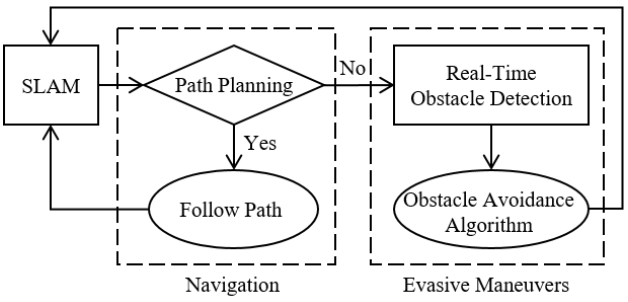

Figure. 1 System model

or structures. This section presents the implementation setup and environment. An indoor environment is selected as the test location as the most realistic and representative situation. The system model of proposed SLAM recovery is shown in Fig. 1.

3.1 Hector SLAM algorithm

Hector SLAM[1] is a 2D SLAM system [9] that incorporates robust LiDAR scan matching and 3D navigation solution, including an expanded Kalman filter (EKF) inertial sensing system. Hector SLAM is based on onboard of actual computations. The six-degree of freedom (6DOF) robot holds highly updated LiDAR-based 2D imaging in real-time while in motion. The Gaussian–Newton optimization method provides the laser beam alignment endpoints with an obtained map, where all prior scans indirectly fit.

The "$Move\_base$" package has used in this study. The "$Move\_base$" node is an important element of the ROS navigation stack. This package enables the UAV to move from its current position to the target position. After the path planning is complete, the user can employ the "$2D\ nav\ goal$" in RVIZ to specify the goal position *(x,y)* and orientation *(x,y),* which will then be published in "$move\_base/goal$" topic.

For "$Move\_base$", a global planner and local navigation planner are available. The global planner calculates a safe route for the UAV to reach the target location. When the UAV starts flying and scans as its moving, the global planner direction is determined. The map is submitted to the local planner until the global planner has prepared the journey. Considering the product of all the laser readings, the local planer splits the route into parts, thereby providing the UAV with speed controls to follow the local direction.

In this study, A* algorithm was used as the global planner and the "$base\_local\_planner$" was used as the trajectory rollout algorithm to calculate the path as a local planner. The A* algorithm can be applied to a grid-type map and the system must recognize surrounding rectangles based on the starting point. Table 1 and Fig. 2 shows the process of A* algorithm. If there are no obstacles, there are eight surrounding points which is shown as rectangles. The system inputs the starting point and surrounding rectangles into Openset. At this time, the starting point or center point is the "Parent" of other Openset. Then, the starting point at Openset is removed and input into the "Visited" so that it does not need to be checked again. In this situation, one of the "Children" (with the smallest f value) is selected and the foregoing process is repeated.

$$f = g + h, \tag{1}$$

Here, g represents the distance from the starting point to the current point and h represents the distance from the current point to the goal point.

The distance from the starting point to the surrounding Openset is 10 and 14. The top, bottom, left and right value is 10 and the diagonal value is 14 from the starting point. The smallest value is assigned as 10. For h, it measures only in a direction other than diagonal and checks the distance between the goal and current points without considering the obstacles. Finally, f is addition of g and h. The rectangle with the smallest f among the Opensets is selected, removed from the Openset and input into "Visited". Additionally, the items in "Visited" (except for obstacles) are placed into Openset and the center is input into the "Parent".

The next rectangle is selected and the surrounding rectangles are input into Openset, while ensuring that there is a rectangle with a smaller g value. If so, the original rectangle is input into "Visited" and converted to a rectangle with a small g value.

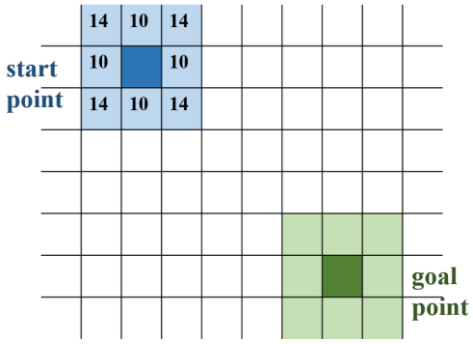

Figure. 2 A * algorithm

Table 1. Process of A * algorithm

	1^{st} **step**	2^{nd} **step**
Openset	center, surrounding 8 rectangles	1^{st} center, surrounding 8 rectangles
Parent	center	center
Openset	surrounding 8 rectangles	1^{st} surrounding 8 rectangles, 2^{nd} surrounding 8 rectangles
Visited	center	1^{st} center, 2^{nd} center

[1] hector slam: http://wiki.ros.org/hector slam

Furthermore, the remainder of the neighborhood is input into Openset. If the destination enters Openset during this repetition, the process can be terminated. Subsequently, the UAV can follow a straight path from the destination, referring to "Visited".

3.2 System setup

The proposed strategy was validated via real-time experiments using the Bebop 2.0 drone. Bebop was selected because of its small size. It can maneuver in dense environments and carry sensor loads. The list of equipment required for the experiment is shown in Table 2. The Jetson TX2 PC has high computational power which can use a 2D LiDAR sensor. The UAV is equipped with this PC and demonstrated in Fig. 3 (c). At the last, stated laptop is used as a ground control station (GCS).

The network architecture of the system is presented in Fig. 3 (a). The UAV is connected with components such as LTE modem, Jetson TX2 and LiDAR sensor. The communication between GCS and UAV is used with wireless systems such as Wi-Fi based and LTE based. All the algorithms were implemented in Python. ROS Kinetic version was used as middleware. The latest version of ROS Bebop autonomy[2] was adopted.

3.3 LTE connection

In this proposed, the UAV can support with LTE connection with softmod. First, the LTE modem attaches to the Parrot Bebop 2 as shown in Fig. 3 (c). Then, configuration is set up to the drone to hijack the mode of Wi-Fi connection to LTE connection. With only Wi-Fi connection (without using LTE), the UAV can fly a maximum distance of 10*m*. In this proposed, LTE was used because if the connection between the UAV and the laptop is lost, the system will stop working. LTE provides greater coverage than Wi-Fi. The Wi-Fi handover scheme for autonomous UAVs was not considered in this study. Additionally, LTE allows multiple UAVs to connect to the GCS. The connection between the GCS and multiple UAVs is based on a ZeroTier server. Fig. 4 (a) illustrates LTE connection between UAV and GCS and Fig. 4 (b) presents the connection between the GCS and multiple UAVs.

3.4 Lidar scanning system

The LiDAR sensor can detect a wider area than the camera and is unaffected by light and weather.

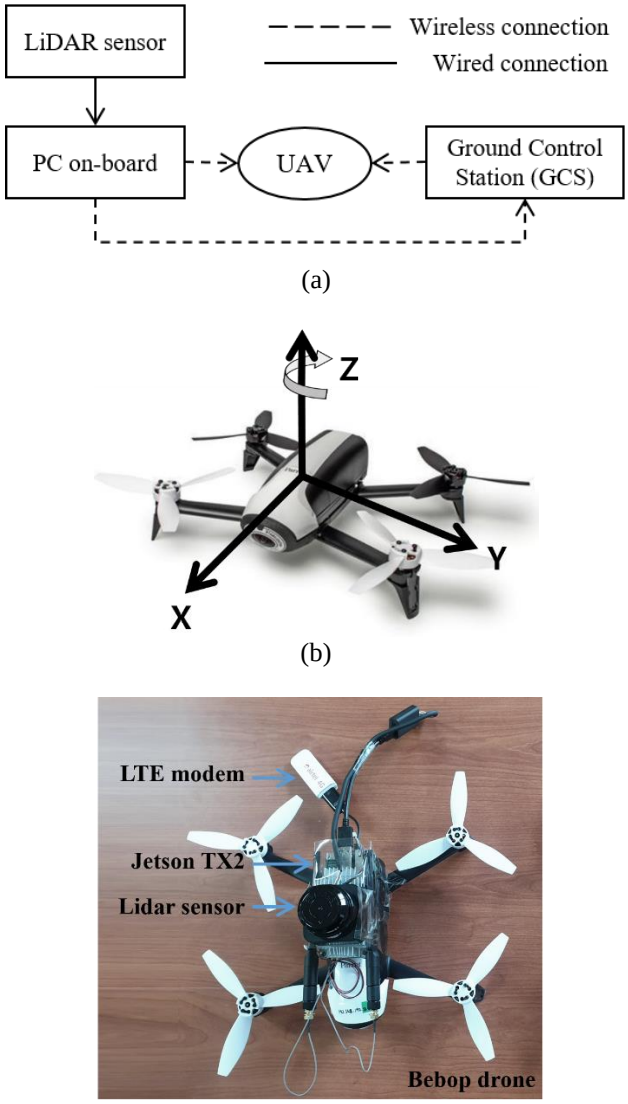

Figure. 3: (a) Network architecture, (b) reference axis and rotation direction for UAV maneuver, and (c) configuration

Table 2. Equipment used

Device	Model name	Company
Lidar sensor	RPLiDAR S1	Slamtec
UAV	Bebop drone 2	Parrot
PC on-board	Jetson TX2	Nvidia
Carrier board	Auvidiea j120	Auvidiea
GCS	ThinkPad T580	Lenovo
LTE modem	LTE USB Stick	Huawei

This characteristic makes UAVs are applicable in both indoor and outdoor environments. The LiDAR sensor used in this study has a measurement range of 360°. Each of the raw laser points is represented in the polar coordinate system as $\{(d_i, \theta_i);\ 0 \leq i \leq 359\}$, where d_i represents the distance from the center

[2] https://bebop-autonomy.readthedocs.io/en/latest/

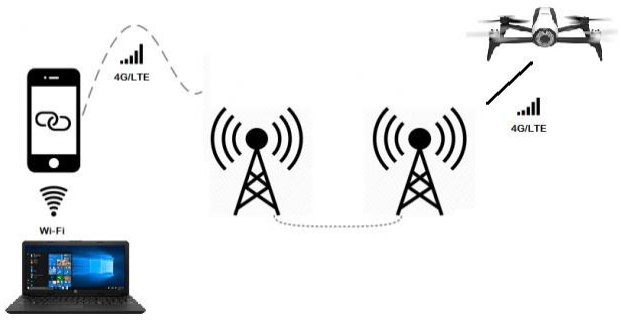

(a)

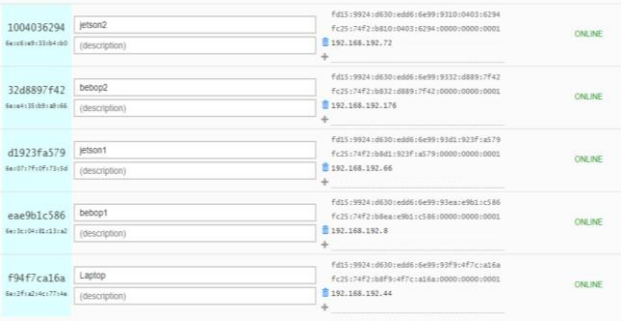

(b)

Figure. 4: (a) Parrot bebop 2 over 4G/LTE (softmod) and (b) zerotier network for multi UAV

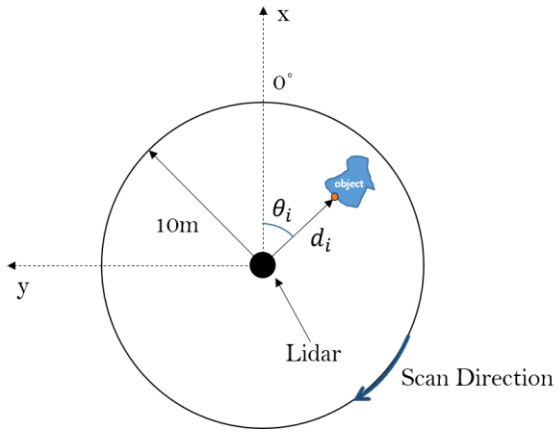

Figure. 5 RPLiDAR S1 scanning system

(a) (b)

Figure. 6 Study room and corridor in kumoh national institute of technology

Algorithm 1: SLAM for obstacle avoidance

```
Result: Avoid obstacle with least space consumption
initialization;
generate map and do localization;
set goal point;
determine obstacle distance value;
while map navigation is generated do
    check path planning;
    if path planning from SLAM is available then
        follow generated path;
    else
        navigation system error;
        Update obstacle position and distance;
        for obstacle distance < r meters do
            check obstacle angle;
            If 0° < obstacle range < θ° then
                rotateleft;
            else
                rotateright;
            end
        end
    end
end
```

Algorithm 1. SLAM for obstacle avoidance

of the UAV to the object and θ_i represents the relative angle of the measurement. The data received by the LiDAR sensor are stored as a vector (d_i θ_i) and checked to convert infinity scan values. The infinity scan values indicate that there is no obstacle from the ray to the maximum range value that can be measured by the LiDAR. Additionally, any object located at the maximum range value (d_{max}) is neglected. In a real-time situation, (d_{max}) do not get infinite value out of the operating range from object. The maximum value of d_i (d_{max}) is 10m for RPLiDAR S1 LiDAR sensor, as depicted in Fig. 5.

3.5 Indoor environment

For the indoor environment, we select a room and a corridor which are shown in Fig. 6. The area is arranged to operate UAV navigation path planning.

3.6 Obstacle avoidance

If path planning is impossible because of temporary errors, the LiDAR sensor continues to attempt obstacle recognition. If an obstacle is recognized, evasive maneuvers are performed through obstacle avoidance control. The pseudo code is followed in Algorithm 1.

4. Implementation result

Obstacle detection in SLAM using based on an accurate map, because inaccurate recognition of the occupied space can cause inefficient evasive trajectory planning. Accordingly, a fast and accurate detection system is required to overcome these issues. The flight results of UAVs during a system error are shown in Fig. 7 (a), indicating the planning path that appears after the target point is selected. However, the UAV may not fly to the planned route because of system error which is shown in Fig. 7 (b).

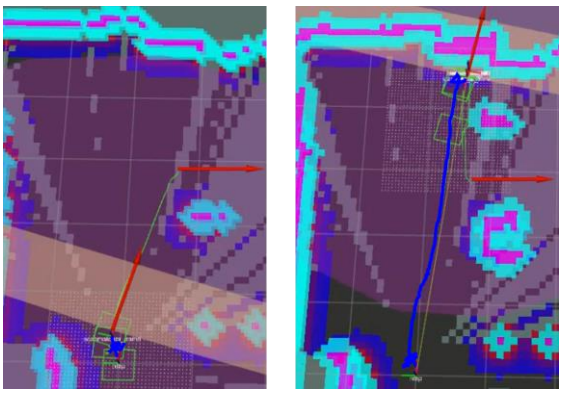

(a) (b)

Figure. 7: (a) Path planning and (b) UAV's movement for navigation system error

(a)

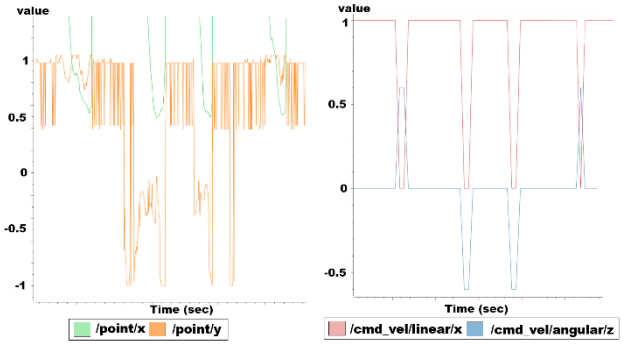

(b) (c)

Figure. 8: (a) The obstacle for avoidance experiment, (b) obstacle position, and (c) UAV's movement for obstacle avoidance

In Fig. 8 (a), it shows an experiment environment for verification of the obstacle avoidance algorithm. Also, Fig. 8 (b) presents the location value of obstacles based on the LiDAR scan information. The movement of UAV for obstacle avoidance using Algorithm 1 is shown in Fig. 8 (c). The UAV rotated in the z-direction of Fig. 3 (b).

The UAV is equipped with a LiDAR sensor producing a 2D point cloud as a metric representation of the environment. A map is updated based on the point cloud in real-time, while the UAV explores the area (see Fig. 9 (a)). While flying in the environment, the UAV can determine its position in a global map

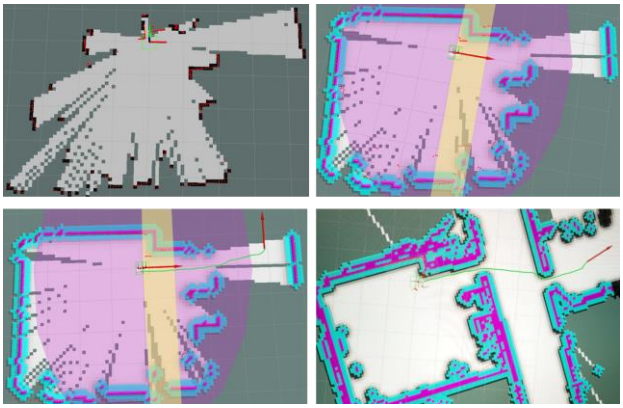

Figure. 9 Left to right and top to bottom: (a) environment mapping, (b) localization on the map, (c) path planning which updated in real-time, and (d) path planning which updated map

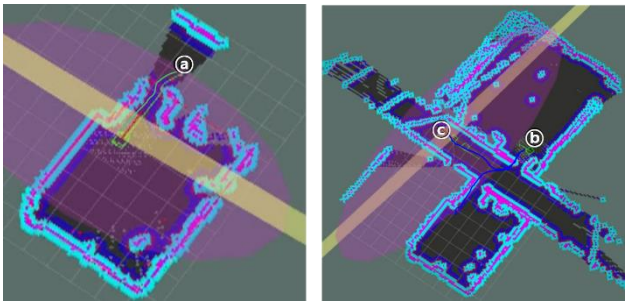

(a) (b)

Figure. 10 Graphical representation of real-time map produced by sensor data: (a) goal point a (b) goal point b and c

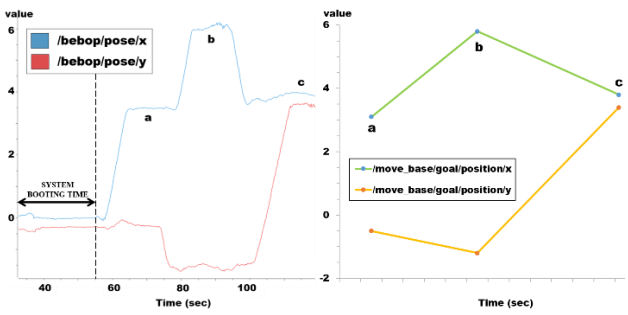

(a) (b)

Figure. 11: (a) UAV's pose and (b) navigation goal

frame, as shown in Fig. 9 (b). Path planning is performed using SLAM to navigate from its current location to the goal point after crossing an obstacle, as depicted in Fig. 9 (c). As shown in Fig. 9 (d), path planning is performed using a previously generated map.

The results have been demonstrated that navigation mapping and time connected with Wi-Fi and LTE. In Fig. 10, it is presented that a real-time map produced by sensor data on the current position using Wi-Fi, which flies through a corridor (a) at a second point (b) and out of the corridor (c) to reach the next point. It is indicated that the axis, blue line and green line are associated with the current location, the flight path of UAV and planned path generated at the designating destination.

These points (a), (b) and (c) are also mentioned in Fig. 11. The real-time position of the x-axis and y-axis of the UAV are shown in Fig. 11 (a) and the navigation goal point which is detected by SLAM at the time is demonstrated in Fig. 11 (b). In the demonstration, the UAV pause on (a) position at 70 seconds because of system booting time. When navigation goal point (a) is expressed at (3.1,-0.5), real position is detected at (3.5, -0.5). At the next goal point (b) is designated at (5.8, -1.2), real position is detected at (6, -1.5). The last goal point is at (3.8, 3.4), UAV is detected at (3.9, 3.6) taking 115 seconds though whole route. An average error rate of position is around (0.23, 0.16).

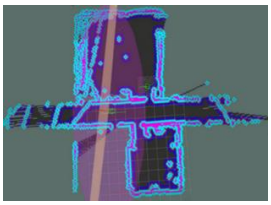

(a)

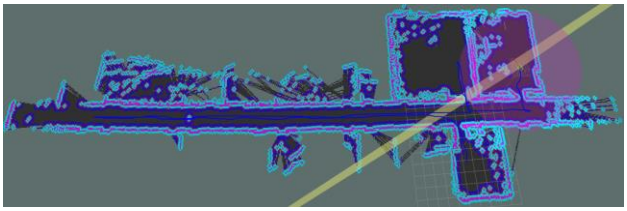

(b)

Figure. 32 Result of map using hector SLAM: (a) Wi-Fi based and (b) LTE based

Table 3. Time of the SLAM navigation using LTE

No.	Take off	Landing
1	0:3.1846	3:12.4515
2	0:3.5811	3:25.2684
3	0:3.7986	3:19.1268
average	0:3.52	3:18.95

In this paper, we have proposed UAV navigation using LTE rather than Wi-Fi because of mapping range. An improved mapping is obtained using the proposed which is presented in Fig. 12 (b) on the experimental environment. The mapping capability of LTE based is 57.5% greater than the Wi-Fi based as shown in Fig. 12 (a). This experiment is summarized in Table 3 on execute time of taking-off and landing. We assume that this map is an unknown area, exploration time is represented as 196 seconds.

The exploration time of the UAV based Wi-Fi was 60 seconds, but a mapping from GCS using Wi-Fi is smaller than using LTE. So it is unnecessary to check and compare exploration time between Wi-Fi based and LTE based.

5. Conclusion

In this paper, we have proposed that a cellular communication-based UAV navigation with obstacle avoidance for unknown indoor environment. The performance of the proposed system is demonstrated in indoor scenarios, considering the UAV movement. It includes obstacle avoidance, UAV pose and navigation goal perspective. In the system, LTE is used for achieving cellular-communication-based connection. Using LTE, wide range of mapping is obtained by UAV on the indoor environment. When cellular communication is used as connection between UAV and GCS, the system has stable connectivity. In the experiment, LTE based increases 57.5% mapping coverage compared with Wi-Fi based. Despite Wi-Fi handover for autonomous UAV is not considered in this paper, LTE based has benefits such as multiple connection between UAV and GCS and connectivity stability.

Conflicts of Interest

The authors declare no conflict of interest.

Author Contributions

“Conceptualization, Yeon Ji Choi and I Nyoman Apraz Ramatryana; methodology, Yeon Ji Choi; software, Yeon Ji Choi; validation, Yeon Ji Choi; writing-original draft preparation, Yeon Ji Choi; writing-review and editing, I Nyoman Apraz Ramatryana; supervision, Soo Young Shin”;

Acknowledgments

“This research was supported by the MSIT (Ministry of Science and ICT), Korea, under the Grand Information Technology Research Center support program (IITP2020-2020-0-01612)

supervised by the IITP (Institute for Information communications Technology Planning Evaluation)".

References

[1] J. Kwak and Y. Sung, "Autonomous UAV Flight Control for GPS-Based Navigation", *IEEE Access*, Vol. 6, pp. 37947-37955, 2018.

[2] Y. Li and C. Shi, "Localization and Navigation for Indoor Mobile Robot Based on ROS", In: Proc. of *2018 Chinese Automation Congress (CAC)*, Xi'an, China, pp. 1135-1139, 2018.

[3] Chen, Derek, and Grace Xingxin Gao, "Probabilistic graphical fusion of LiDAR, GPS, and 3D building maps for urban UAV navigation", *Navigation*, Vol. 66, No. 1, pp.151-168, 2019.

[4] B. Wu, X. Ge, L. Xie, and W. Chen, "Enhanced 3D Mapping with an RGB-D Sensor via Integration of Depth Measurements and Image Sequences", *Photogrammetric Engineering & Remote Sensing*, Vol. 85, No. 9, pp. 633-642, 2019.

[5] X. Lin, J. Wang, and C. Lin, "Research on 3D Reconstruction in Binocular Stereo Vision Based on Feature Point Matching Method", In: *Proc. of 2020 IEEE 3rd International Conf. on Information Systems and Computer Aided Education (ICISCAE)*, Dalian, China, pp. 551-556, 2020.

[6] Panchpor, A. Aishwarya, Sam Shue, and James M. Conrad, "A survey of methods for mobile robot localization and mapping in dynamic indoor environments", In: *Proc. of 2018 Conf. on Signal Processing and Communication Engineering Systems (SPACES)*, Vijayawada, India, pp. 138-144, 2018.

[7] H. Wang, M. Huang, and D. Wu, "A Quantitative Analysis on Gmapping Algorithm Parameters Based on Lidar in Small Area Environment", In: *Proc. of Chinese Intelligent Systems Conf.* Springer, Singapore, pp. 480-492, 2019.

[8] W. Hess, D. Kohler, H. Rapp, and D. Andor, "Real-time loop closure in 2d lidar slam", In: *Proc. of 2016 IEEE International Conf. on Robotics and Automation (ICRA)*, Stockholm, Sweden, pp. 1271-1278, 2016.

[9] P. Vanicek and L. Beran, "Navigation of robotics platform in unknown spaces using LIDAR, Raspberry PI and hector slam", *Journal of Fundamental and Applied Sciences*, Vol. 10, No. 3S, pp. 494-506, 2018.

[10] I. Z. Ibragimov and I. M. Afanasyev, "Comparison of ROS-based visual SLAM methods in homogeneous indoor environment", In: *Proc. of 2017 14th Workshop on Positioning, Navigation and Communications (WPNC)*, Bremen, Germany, pp. 1-6, 2017.

[11] M. Filipenko and I. Afanasyev, "Comparison of various slam systems for mobile robot in an indoor environment", In: *Proc. of 2018 International Conf. on Intelligent Systems (IS)*, Funchal, Madeira Island, pp. 400-407, 2018.

[12] J. M. Santos, D. Portugal, and R. P. Rocha, "An evaluation of 2D SLAM techniques available in robot operating system", In: *Proc. of 2013 IEEE International Symposium on Safety, Security, and Rescue Robotics (SSRR)*, Linkoping, Sweden, pp. 1-6, 2013.

[13] M. Rojas-Fernandez, D. Mujica-Vargas, M. Matuz-Cruz, and D. Lopez-Borreguero, "Performance comparison of 2D SLAM techniques available in ROS using a differential drive robot", In: *Proc. of 2018 International Conf. on Electronics, Communications and Computers (CONIELECOMP)*, Cholula Puebla, Mexico, pp. 50-58, 2018.

[14] D. Mellinger and V. Kumar, "Minimum snap trajectory generation and control for quadrotors", In: *Proc. of 2011 IEEE International Conf. on Robotics and Automation*, Shanghai, China, pp. 2520-2525, 2011.

[15] D. Mellinger, N. Michael, and V. Kumar, "Trajectory generation and control for precise aggressive maneuvers with quadrotors", *The International Journal of Robotics Research*, Vol. 31, No. 5, pp. 664-674, 2012.

[16] P. Checchin, F. Gerossier, C. Blanc, R. Chapuis, and L. Trassoudaine, "Radar scan matching slam using the fourier-mellin transform", *Field and Service Robotics*, Vol. 62, pp. 151-161, 2010.

[17] J. Engel, T. Schops, and D. Cremers, "LSD-SLAM: Large-scale direct monocular SLAM", In: *Proc. of European Conf. on Computer Vision, Springer*, Zurich, Switzerland, pp. 834-849, 2014.

[18] G. Sibley, C. Mei, P. Newman, and I. Reid, "A system for large-scale mapping in constant-time using stereo", *International Journal of Robotics Research*, pp. 834-849, 2010.

[19] M. Muller, S. Lupashin, and R. D'Andrea, "Quadrocopter ball juggling", In: *Proc. of 2011 IEEE/RSJ International Conf. on Intelligent Robots and Systems*, San Francisco, California, USA, pp. 5113-5120, 2011.

[20] T. C. Wang, C. S. Tong, and B. L. Xu, "AGV navigation analysis based on multi-sensor data fusion", *Multimedia Tools and Applications*, Vol. 79, No. 7, pp. 5109-5124, 2020.

[21] T. Pozderac, J. Velagić, and D. Osmanković, "3D Mapping Based on Fusion of 2D Laser and IMU Data Acquired by Unmanned Aerial Vehicle", In: *Proc. of 2019 6th International Conf. on Control, Decision and Information Technologies (CoDIT)*, Paris, France, pp. 1533-1538, 2019.

[22] F. Huang, H. Yang, X. Tan, S. Peng, J. Tao, and S. Peng, "Fast Reconstruction of 3D Point Cloud Model Using Visual SLAM on Embedded UAV Development Platform", *Remote Sensing*, Vol. 12, No. 20, pp. 3308, 2020.

[23] A. Bachrach, R. He, and N. Roy, "Autonomous flight in unknown indoor environments", *International Journal of Micro Air Vehicles*, Vol. 1, No. 4, pp. 217-228, 2009.

[24] M. Achtelik, M. Achtelik, S. Weiss, and R. Siegwart, "Onboard IMU and monocular vision based control for MAVs in unknown in-and outdoor environments", In: *Proc. of 2011 IEEE International Conf. on Robotics and Automation*, Shanghai, China, pp. 3056–3063, 2011.

[25] M. Blosch, S. Weiss, D. Scaramuzza, and R. Siegwart, "Vision based MAV navigation in unknown and unstructured environments", In: *Proc. of 2010 IEEE International Conf. on Robotics and Automation*, Anchorage, Alaska, USA, pp. 21-28, 2010.

[26] F. Liu, J. Liu, Y. Yin, W. Wang, D. Hu, P. Chen, and Q. Niu, "Survey on WiFi-based indoor positioning techniques", *IET Communications*, Vol. 14, No. 9, pp. 1372-1383, 2020.

[27] J. Kwak and Y. Sung, "Beacon-Based Indoor Location Measurement Method to Enhanced Common Chord-Based Trilateration", *Journal of Information Processing Systems*, Vol. 13, No. 6, pp. 1640-1651, 2017.